ACS OMEGA

Article

Cite This: ACS Omega 2019, 4, 4793−4803

http://pubs.acs.org/journal/acsodf

Carboxymethyl Cellulose−Xylan Hydrogel: Synthesis, Characterization, and in Vitro Release of Vitamin B_{12}

Debashis Kundu and Tamal Banerjee*

Department of Chemical Engineering, Indian Institute of Technology Guwahati, Guwahati 781039, Assam, India

Supporting Information

ABSTRACT: The current work reports the synthesis of carboxymethyl cellulose (CMC) and xylan-based homopolymerized as well as copolymerized hydrogels using an ethylene glycol diglycidyl ether cross-linker in alkaline medium. The hydrogels are physically characterized by the swelling ratio and gel fraction. The morphological observation of hydrogels reveals the porous structure for the copolymerized gels. The rheological behavior of the gels elaborates that the copolymerized CMC−xylan gel synthesized in a 1:1 molar ratio has superior strain-bearing ability and possesses the shortest gelation temperature and time. Vitamin B_{12} here is used as the model vitamin to be loaded in the hydrogels and subsequent studies involving the in vitro release in artificial gastric fluid (AGF, pH = 1.2), artificial intestinal fluid (AIF, pH = 6.8), and phosphate-buffered saline (PBS, pH = 7.4). The synthesized gels show a cumulative release of 19−28% in AGF, 80−88% in AIF, and 93−98% in PBS, independently. Further, the highest cumulative release of 93−99% is recorded for all gels when in vitro release is performed in successive buffers, that is, first in AGF, followed by AIF and PBS.

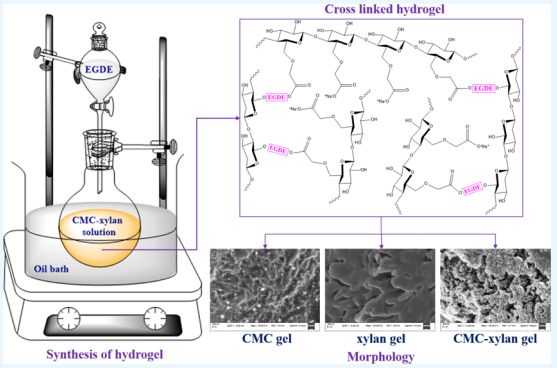

1. INTRODUCTION

Hydrogels are physical or chemical cross-linked three-dimensional polymer networks which swell upon absorbing water but do not dissolve in it. The network often mimics the extracellular matrix and is thus widely used in drug delivery, tissue engineering, and other biological applications.[1] The shape and volume of hydrogels can be reversibly changed upon various external stimuli such as pH, temperature, light, electric and magnetic fields. Polysaccharides are renewable natural polymers bearing the advantages which include nontoxicity, biocompatibility, biodegradability, and natural abundance. The ease of functionalization or chemical cross-linking of the hydroxyl moieties present in the backbone of polysaccharides make them attractive precursors for hydrogels.

Carboxymethyl cellulose (CMC) is a water-soluble derivative of cellulose in which some of the hydroxyl moieties are replaced by carboxymethyl moiety. It is conveniently produced by the alkali-catalyzed reaction between cellulose and chloroacetic acid. It is widely used as thickener, viscosity modifier, emulsion stabilizer, and water retention agent in paint, cosmetic, and food industries. Low immunogenicity, high biocompatibility, and biodegradability make it a potential carrier for controlled release or site-specific drug delivery.[2,3] For this, it got approval from FDA for biomedical applications.[4] CMC is also used as a precursor for stimuli-responsive hydrogels. The carboxymethyl group adds a negative charge to the pyranose backbone, and it significantly increases the cross-linking points and reactive sites. Thus, thermal radical reactions are often employed with the cross-linker to prepare CMC-based homopolymer and copolymer hydrogels.[5,6] Overall, the CMC-based hydrogels are used as carriers for drugs and biological macromolecules.[7]

Xylan is a heteropolysaccharide consisting of pentoses and hexoses. It belongs to the hemicellulose family and found in most abundant quantity in the family. Xylan consists of 80−200 D-xylopyranosyl residues as backbone, which are connected by β-(1 → 4) glycosidic bonds.[8] The backbone is linked with the *O*-acetyl, glucoronic acid side groups.[9] Xylan is obtained from hardwood by the alkali extraction method. Like cellulose, hemicellulose as well as xylan can be easily functionalized because of the abundance of the hydroxyl moiety. The various subclasses of hemicellulose are used as thickeners, emulsifiers, coatings, and additives in paper, food, and pharmaceutical industries.[10,11] Recently, xylan-based hydrogels have gained attention because of the multiresponsive behavior toward pH, organic solvents, and ions. A good number of literature is available for the xylan-based hydrogels as carriers for drug and biological macromolecules[12] and sorbents for heavy metal ions and organic dyes.[13,14]

Vitamin B_{12} (VB_{12}, cyanocobalamin) is the largest and the most complex in the vitamin family. It is an organometallic compound containing cobalt within a corrin ring. The main residues are corrin ring, propyl side chain, ribose group, and dimethylbenzimidazole. Because of its low bioavailability (recommended 1−5 μg per day), it is considered as an essential

Received: December 30, 2018
Accepted: February 20, 2019
Published: March 4, 2019

DOI: 10.1021/acsomega.8b03671
ACS Omega 2019, 4, 4793−4803

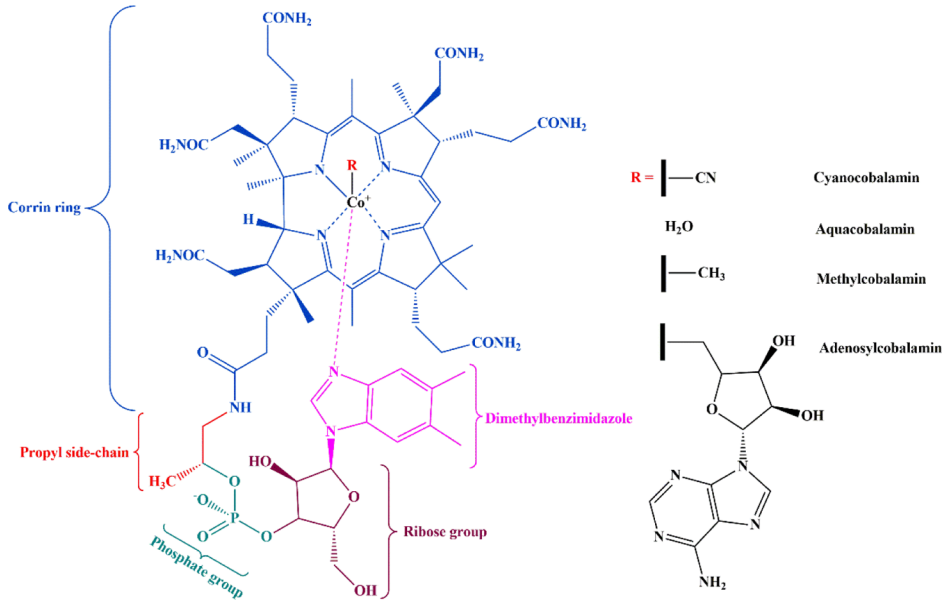

Figure 1. Structure of VB_{12}.[15]

nutrient. The different chemical structures of cyanocobalamin and its derivatives are shown in Figure 1. Two of the major active forms are methylcobalamin and adenosylcobalamin. Methylcobalamin is needed by methionine synthase to produce the amino acid methionine from homocysteine, whereas adenosylcobalamin is used as a cofactor by methylmalonyl−coenzyme A to produce succinyl coenzyme A, which is required to enter the tricarboxylic acid cycle.[15] Aquacobalamin bears a neutral ligand that results in a positively charged molecule and is therefore always accompanied by a counter anion.[16] The deficiency of cobalt in human is treated with the controlled release of VB_{12} which increases the concentration level of cobalt in blood serum and liver. The ribose group plays an important role in the synthesis of nucleic acids and the reduction of ribonucleotides to deoxyribonucleotides. Jin et al. reported that VB_{12} is prescribed to alleviate the symptoms of megaloblastic anemia, allergic asthma, and allergic rhinitis.[17] Further, the sustained level of VB_{12} eases the pain associated with carpal tunnel syndrome. The deficiency can lead to weakness, fatigue, constipation, and other neurological malfunctions.[18]

A moderate number of literature is available for the controlled release of various vitamins including VB_{12}. To the best of our knowledge, the earliest reported VB_{12} release was by using cross-linked poly(*N*-vinyl-2-pyrrolidone) polyacrylamide and acrylic acid-based hydrogels.[19,20] A more recent investigation on the diffusion mechanism of VB_{12} was studied by Jin et al.[17] using poly(acrylic acid) and copolymeric acrylic acid and *N*-vinyl pyrrolidinone-based hydrogels. Further Maheswari et al. investigated the release profile of VB_{12} using thermosensitive poly(*N*-isopropylacrylamide-*co*-*N*-vinyl-2-pyrrolidinone) hydrogels.[21] CMC-based hydrogels are recently being explored for the release of VB_{12}. Boruah et al. reported the in vitro release of VB_{12} using CMC-grafted poly(acrylic acid) and organophilic montmorillonite nanoclay composite hydrogel.[22] Further, Nath and Dolui reported CMC-grafted poly(acrylic acid) and layered double hydroxide (LDH) hydrogels for the in vitro release study of VB_{12}.[23] Multiresponsive xylan-based hydrogels are reported by Cao et al. for the release of VB_{12}.[24] The hydrogel is formed with xylan-type hemicellulose methacrylate and 4-[(4-acryloyloxyphenyl)azo]benzoic acid, using the free-radical copolymerization method.

Herein, we have synthesized pure CMC, pure xylan hydrogels, and CMC−xylan hydrogels in different molar ratios. The interconnected cross-linked structure is fabricated using an ethylene glycol diglycidyl ether (EGDE) cross-linker. The hydrogels are characterized by Fourier transform infrared (FT-IR) spectroscopy, and the morphology of the hydrogels is viewed by an optical microscope and a field emission scanning electron microscope. The rheological behavior of the as-synthesized hydrogels is performed at 25 °C. By varying the shear rate in a wide range, the viscosity of the gels is measured. Frequency sweep is used to observe the detailed viscoelastic behavior of the gels as well as to measure the gel point of the hydrogels. Thereafter, temperature sweep is performed to identify the gelation temperature. The time sweep then determines the gelation time. Swelling ratios (SRs) at various pHs and gel fractions are measured to determine the physical characteristics of the gel. To the best of our knowledge, this is the first attempt to prepare a chemically cross-linked cellulose−hemicellulose-based hydrogel. VB_{12} is used as a model vitamin to be loaded in the hydrogels. The in vitro release of VB_{12} is carried out in artificial gastric fluid (AGF, pH = 1.2), artificial intestinal fluid (AIF, pH = 6.8), and phosphate-buffered saline (PBS, pH = 7.4).

2. MATERIALS AND METHODS

2.1. Materials. The CMC sodium salt and beechwood xylan (xylan) were purchased from Sigma-Aldrich. Auxiliary chemicals such as sodium hydroxide, sodium chloride, potassium dihydrogen phosphate, and hydrochloric acid (37 wt %) were purchased from Merck. EGDE and vitamin B_{12} were purchased from TCI India. PBS was purchased from HiMedia. All the chemicals were used as received. Deionized (DI) water was supplied from the in-house Millipore water synthesis unit (make: Millipore, model: ELix-3).

2.2. Preparation of Hydrogels. The synthesis of hydrogels is divided into three distinct steps, namely (i) preparation of precursors, (ii) synthesis of hydrogels by the addition of cross-linkers, and (iii) purification of hydrogels. The schematic of the

DOI: 10.1021/acsomega.8b03671
ACS Omega 2019, 4, 4793−4803

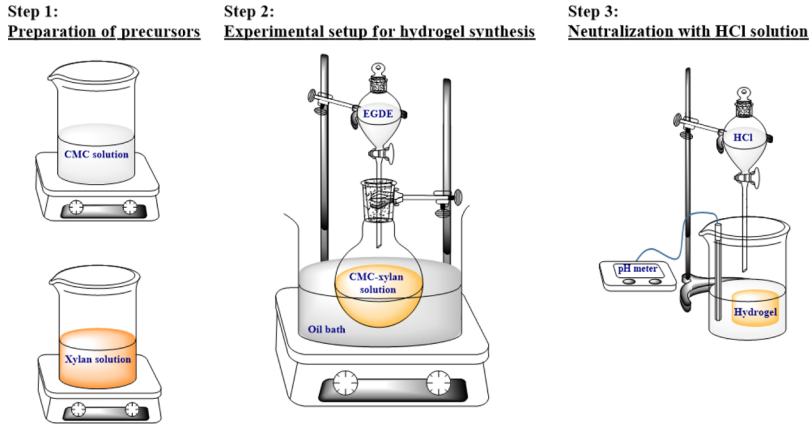

Figure 2. Schematic of hydrogel synthesis.

three steps are given in Figure 2. In the first step, the precursor solutions of CMC and xylan were separately dissolved in 1 mol L^{-1} aqueous NaOH solution. After obtaining homogeneous solutions, xylan and CMC were mixed in 25:75 mol % (hereby denoted as XC25), 50:50 mol % (hereby denoted as XC50), and 75:25 mol % (hereby denoted as XC75), respectively. Next, the solutions were transferred into round-bottom flasks and then heated to 50 °C to get homogeneous mixtures. The EGDE cross-linker was added dropwise into the solutions. Gelation was seen to complete within 15 min. After the formation of gels, they were thoroughly washed with DI water to remove the unreacted monomers and the cross-linker. Thereafter, they were neutralized with 0.1 M HCl solution and subsequently lyophilized for further characterization (freeze dryer, make: Martin Christ, model: Alpha 2-4 LD). In addition to the copolymerized CMC−xylan gel, EGDE was also added dropwise into pure xylan and pure CMC solutions to prepare pure xylan (hereby denoted as xylan gel) and pure CMC (hereby denoted as CMC gel), respectively. The cross-linking scheme of the hydrogels is given in Figure 3.

2.3. Characterization. *2.3.1. FT-IR Spectroscopy.* The hydrogels were grinded and mixed with an excess amount of dried potassium bromide (KBr). Later, the mixed powder was placed in a hydraulic press to prepare transparent pellets. The pellets were placed in an FT-IR spectrometer (make: Shimadzu, model: IRAffinity-1), and the transmission spectra were recorded within the range of 400−4000 cm^{-1} using 30 scans per sample with a resolution of 4 cm^{-1}.

2.3.2. Morphology. The morphology of the hydrogels was observed with an optical microscope (make: Carl Zeiss, model: Scope A1, AXIO, software: ZEN 2.3) and a field emission scanning electron microscope (make: Carl Zeiss, model: GeminiSEM 300). For optical microscopic images, the freeze-dried hydrogels were placed on a glass slide and covered with a coverslip. For field emission scanning electron microscopy (FESEM) images, the hydrogels were placed on a carbon tape and placed on a stub. The stub was later sputter-coated with gold. The measurement was carried out at a potential of 3 kV at an optical zoom of 1 μm and 200 nm.

2.3.3. Rheology. The rheological studies of hydrogels were performed on a rheometer (make: Anton Paar (Austria), model: Physica MCR 301) using cone-and-plate geometry (diameter: 50 mm, angle: 1°, 0.1 mm gap) at 25 °C. The flow behavior of the hydrogels was determined within a shear rate of 1×10^{-2} to 1×10^{3} s^{-1}. To find the storage moduli (G'), loss moduli (G''), and linear viscoelastic region (LVR) profiles, amplitude test was performed at a constant angular frequency of 1 Hz and within a strain of 1×10^{-1} to 1×10^{3}%. Frequency sweep test of the gels was performed at a constant strain of 1% within a frequency of 1×10^{-2} to 1×10^{3} Hz. The constant strain of 1% is obtained from LVR. The loss tangent ($\tan \delta$) is determined from the loss and storage moduli obtained from the frequency sweep test and is defined as the ratio of viscous to elastic response. The expression is given as

$$\tan \delta = \frac{G''}{G'} \tag{1}$$

The temperature sweep of the precursor solution was performed at a temperature range of 25−80 °C with 1% of strain obtained from LVR and with 1 Hz frequency obtained from the frequency sweep test. The time sweep of the precursor solution was performed for 60 min at the corresponding gelation temperature with 1% of strain obtained from LVR and with 1 Hz frequency obtained from the frequency sweep test.

2.3.4. Equilibrium Swelling Ratio. Swelling determines the amount of water absorbed by the hydrogel within a certain period. We determined the equilibrium SR of the hydrogel, that is, the highest amount of water absorbed by the hydrogel after attaining equilibrium weight. Briefly, a certain amount of freeze-dried hydrogel was submerged into the pH buffer or DI water for 48 h at 25 °C. The hydrogel was allowed to swell inside the buffer or DI water to attain equilibrium. After 48 h, the hydrogel was filtered to remove the excess water, after which the weight was measured. The equilibrium SR is measured as

$$\text{SR}\ (\%) = \frac{(W_{eq} - W_i)}{W_i} \times 100\% \tag{2}$$

where W_i is the weight of the freeze-dried hydrogel and W_{eq} is the equilibrium weight of the hydrogel. The swelling was measured in AGF (pH = 1.2), AIF (pH = 6.8), PBS (pH = 7.4), and DI water. The pHs of the solutions were adjusted by a digital pH meter (make: Eutech Instruments, model: EUTECH pH700).

2.3.5. Gel Fraction. Gel fraction was calculated as described in the literature.[25] Fridge-dried hydrogel was heated at 60 °C for 24 h, and the weight was measured (W_0). Therefore, the hydrogel was immersed in DI water to remove the soluble parts and heated at 121 °C for 4 h. The excess amount of water was filtered and further dried at 60 °C for 72 h. The final weight was measured as W_1. The gel fraction is then given by

DOI: 10.1021/acsomega.8b03671
ACS Omega 2019, 4, 4793−4803

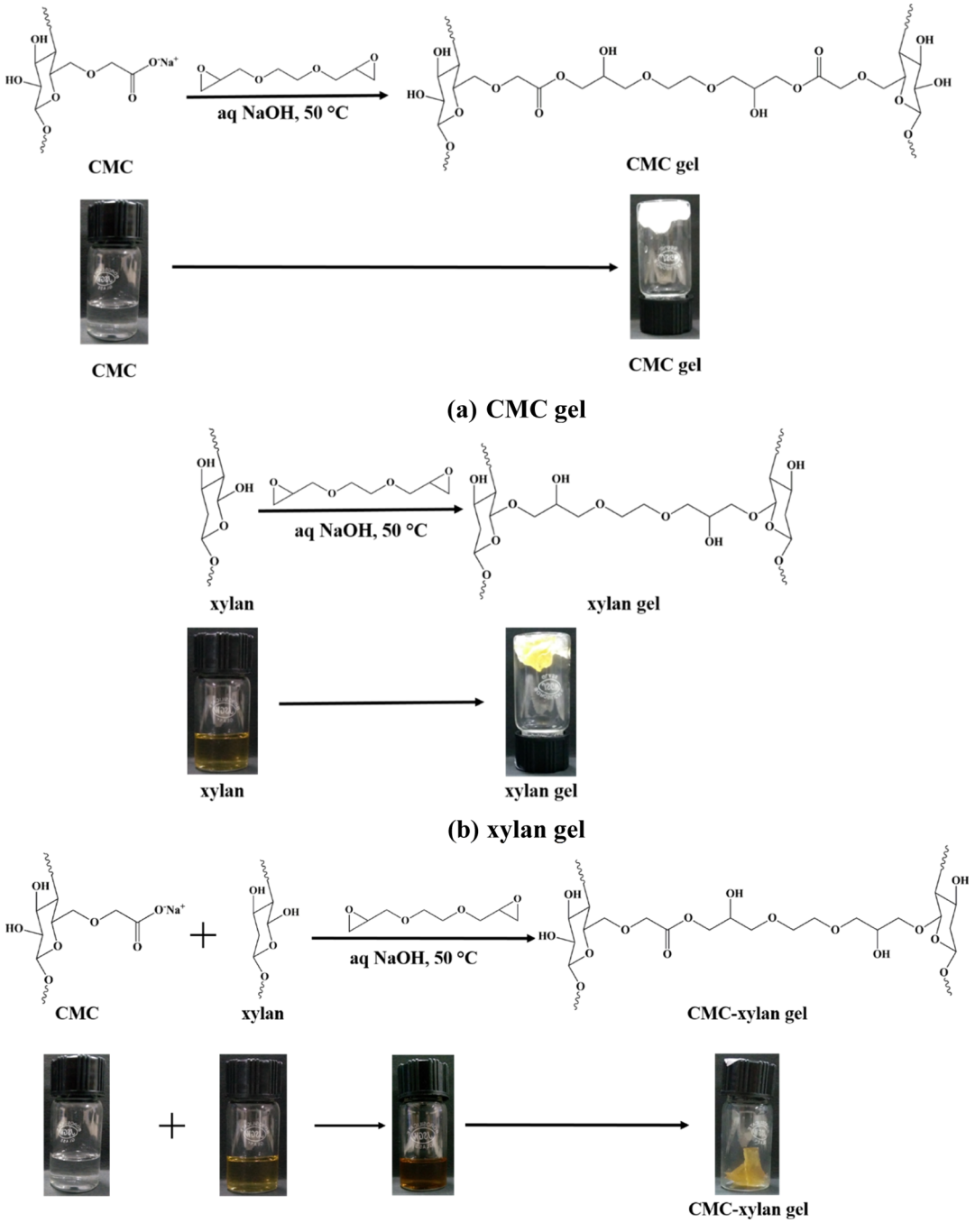

Figure 3. Reaction scheme of the hydrogel formation: (a) CMC gel, (b) xylan gel, and (c) CMC−xylan gel.

$$\text{gel fraction (\%)} = \left(\frac{W_1}{W_0}\right) \times 100\% \quad (3)$$

Both equilibrium SR and gel fraction measurements were performed in triplicate, and the standard deviation is represented in terms of error bars.

2.4. Loading of VB_{12}. Preweighed amounts of freeze-dried hydrogels were immersed in 20 mL of VB_{12} solution (0.5 mg mL^{-1}). The sample tubes were kept in an orbital shaker (make: Daihan Labtech, model: LSI 3016R) for 48 h at 25 °C (±0.5 °C) and 120 rpm under dark conditions. After 48 h, the tubes were placed in a centrifuge at 10 000 rpm to obtain clear supernatants. Later, the samples were filtered to separate the vitamin-loaded gels and the supernatants. Later, the vitamin-loaded gels were freeze-dried. An appropriate volume of the supernatant was collected and appropriately diluted to measure the concentration of the remaining VB_{12} by UV−vis spectroscopy. The amount of vitamin loaded in the hydrogel (VB_{12} loading) is calculated by[26]

$$VB_{12}\text{ loading (\%)} = \frac{\text{amount of } VB_{12} \text{ in hydrogel}}{\text{amount of freeze-dried hydrogel}} \times 100 \quad (4)$$

DOI: 10.1021/acsomega.8b03671
ACS Omega 2019, 4, 4793−4803

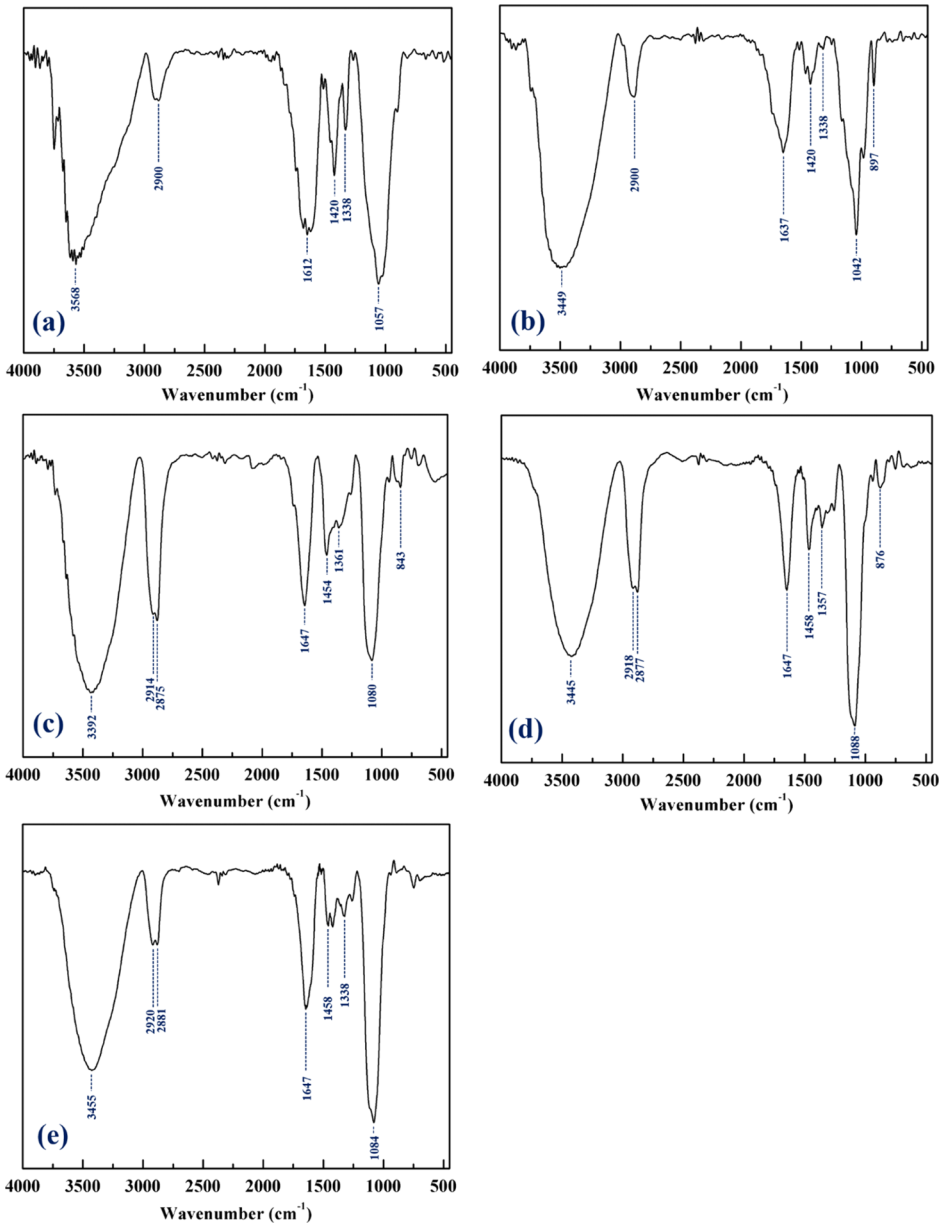

Figure 4. FT-IR spectra: (a) pure CMC, (b) pure xylan, (c) CMC gel, (d) xylan gel, and (e) CMC−xylan.

2.5. Preparation of AGF and AIF. AGF was prepared by adding 2.0 gm of sodium chloride and 7.0 mL of hydrochloric acid (37 wt %) in a 1000 mL volumetric flask. The final volume was made up to 1000 mL by adding DI water until the pH became 1.2. AIF was prepared by dissolving 6.8 gm of potassium dihydrogen phosphate in 500 mL of DI water. The pH of the solution was adjusted to 6.8 and the final volume of the solution was made upto 1000 mL. Both the preparation methods are duly adopted from the literature.[27]

2.6. Release of VB_{12}. The release of VB_{12} was carried out in three buffers, namely, AGF, AIF, and PBS, respectively. The VB_{12}-loaded dried hydrogels were placed in buffers, and 20 mL of the buffer solution was added. The solutions were placed in the same orbital shaker at 37 °C (±0.5 °C) at 60 rpm. After each hour, 5 mL of the buffer solution was collected and replaced by 5 mL of fresh buffer solution to maintain equal volume. The method of collection of aliquots has also been adopted from the literature.[5] The collected aliquots were filtered to remove any fragment of the hydrogel. The amount of VB_{12} in the aliquots was determined by UV−vis spectroscopy.

2.7. UV−Vis Spectroscopy. The concentration of VB_{12} in the supernatant solutions and aliquots was measured against the standard calibration curve. The calibration curve was plotted with the absorbance values of VB_{12} solutions against the known concentrations of VB_{12}. The known concentrations were prepared by appropriate dilutions of the stock VB_{12} solution (1 mg mL^{-1}). Thereafter, the absorbance of the supernatant solutions and aliquots were measured with a UV−vis spectrophotometer (make: Shimadzu, model: UV-2600). Separate calibration curves were plotted for AGF, AIF, PBS buffers (for the aliquots), and DI water (for the supernatants).

3. RESULTS AND DISCUSSION

3.1. FT-IR Spectra. Figure 4 represents the FT-IR characterization of pure CMC, pure xylan, synthesized CMC gel, xylan gel, and CMC−xylan gel. The major characteristic

DOI: 10.1021/acsomega.8b03671
ACS Omega 2019, 4, 4793−4803

peaks of CMC and xylan are O−H stretching, C−H stretching, C−O stretching, C−H bending, C−C bending, skeletal vibrations of C−O and C−C in the pyranose ring, antisymmetric β-(1 → 4) glycosidic linkage, and C−H glycosidic deformation. The FT-IR spectra of pure CMC and pure xylan are shown in Figure 4a,b. The O−H stretching of pure CMC and pure xylan are assigned at 3568 and 3449 cm^{-1}, respectively. The C−H stretchings of both are assigned at 2900 cm^{-1}. The stretching of C−O is assigned at 1612 cm^{-1} for pure CMC and 1637 cm^{-1} for pure xylan. The bending of $-CH_2$ is assigned at 1420 cm^{-1} for both cases. The skeletal vibrations are also observed at 1320 and 1338 cm^{-1}, respectively. For pure CMC, the bending of C−C is assigned at 1057 cm^{-1}, and the same for pure xylan is assigned at 1042 cm^{-1}.

The characteristic peaks in the FT-IR spectra of CMC gel, xylan gel, and CMC−xylan gel (Figure 4c−e) are found in similar positions. For the hydrogels, the stretching of O−H varies in the range of 3392−3455 cm^{-1}. A doublet peak of 2914−2920 and 2875−2881 cm^{-1} represents C−H stretching and bending, respectively. C−O stretching is assigned at 1647 cm^{-1}. The bending of $-CH_2$ is assigned at 1454−1458 cm^{-1}. The skeletal vibrations are shifted in the range of 1338−1361 cm^{-1}. Kono et al. report the bending of C−C at 1064 cm^{-1},[28] and Sekkal et al. report the antisymmetric β-(1 → 4) glycosidic linkage at 1090 cm^{-1}.[29] For this, the broad peak at 1080−1088 cm^{-1} is collectively considered as the merger of antisymmetric β-(1 → 4) glycosidic linkage and bending of C−C. The glycosidic deformation of C−H with ring vibration is assigned at 843−876 cm^{-1}.

3.2. Morphology of Hydrogels. The morphology of the hydrogels visualized by a field emission scanning electron microscope and an optical microscope is shown in Figures 5 and 6, respectively. From the FESEM images (Figure 5), the microstructure of the xylan gel appears to be coarse in nature

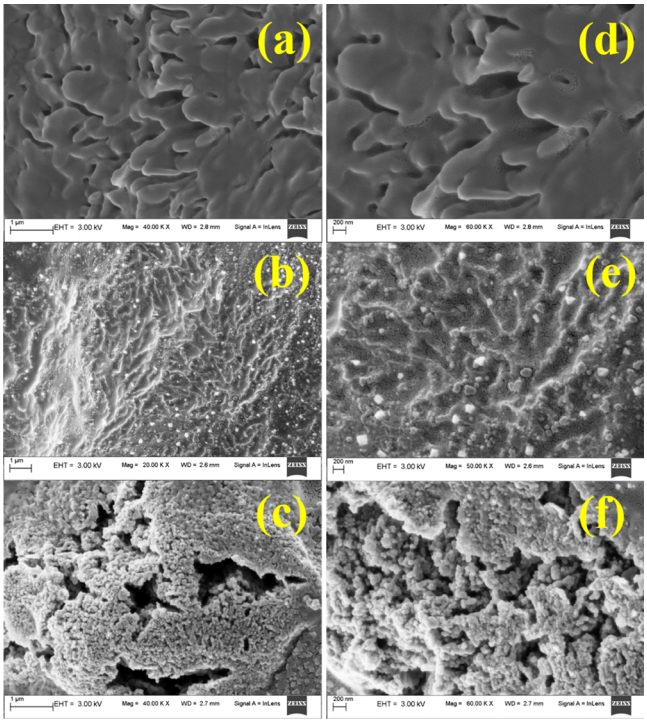

Figure 5. FESEM morphology of hydrogels at 1 μm (a−c) and 200 nm (d−f). (ad) Xylan gel, (b,e) CMC gel, and (c−f) CMC−xylan gel.

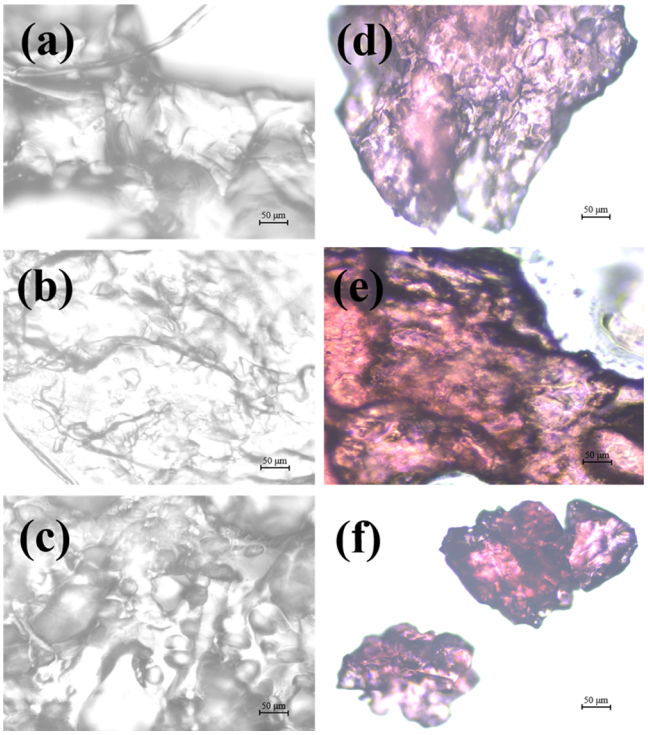

Figure 6. Optical microscope images of hydrogels (a−c) and VB_{12}-loaded hydrogels (d−f). (a,d) Xylan gel, (b,e) CMC gel, and (c,f) CMC−xylan gel.

with random elongations. The random elongations create uneven pores and an increased surface area which may act as possible complex formation sites for VB_{12}. In contrast to the xylan gel, CMC gel appears to have an uneven surface only. The beads visible on the surface may be the sodium ions of the CMC sodium salt. The presence of sodium ions on the surface reflects the presence of carboxymethyl chains attached to the pyranose ring of CMC, and for this reason VB_{12} easily binds with the CMC gel. However, the copolymerized CMC−xylan gel has a porous structure. The pores are well-attributed to absorb VB_{12} inside the pore wall, enabling a higher uptake of VB_{12}. The hydrogels appear to be glossy and coarse in the optical microscopic images (Figure 6a−c). The VB_{12}-loaded hydrogels are further visualized using an optical microscope and are given in Figure 6d−f. Upon loading of VB_{12}, the hydrogels do not lose their glossy appearance, and the vitamin is seen to absorb throughout the surface.

3.3. Rheological Analysis. The rheological behavior of hydrogels is displayed in Figure 7. The viscosity of the gels is measured at 25 °C within a shear rate of 0.01−1000 s^{-1} and is shown in Figure 7a. For all the hydrogels, with an increasing shear rate, the viscosity decreases, referring to the shear-thinning behavior of the hydrogels. At a high rate (>100 s^{-1}), the viscosities of all hydrogels are found in a similar region, although the distinct nature of curves is visible at a lower shear rate. This is attributed to the loosening of the cross-linking structure at a high shear rate. The shear-thinning behavior of the hydrogels is further confirmed by fitting the flow behavior in the power-law model.

The power-law equation in terms of apparent viscosity is

$$\eta = m(\dot{\gamma})^{n-1} \quad (5)$$

DOI: 10.1021/acsomega.8b03671
ACS Omega 2019, 4, 4793−4803

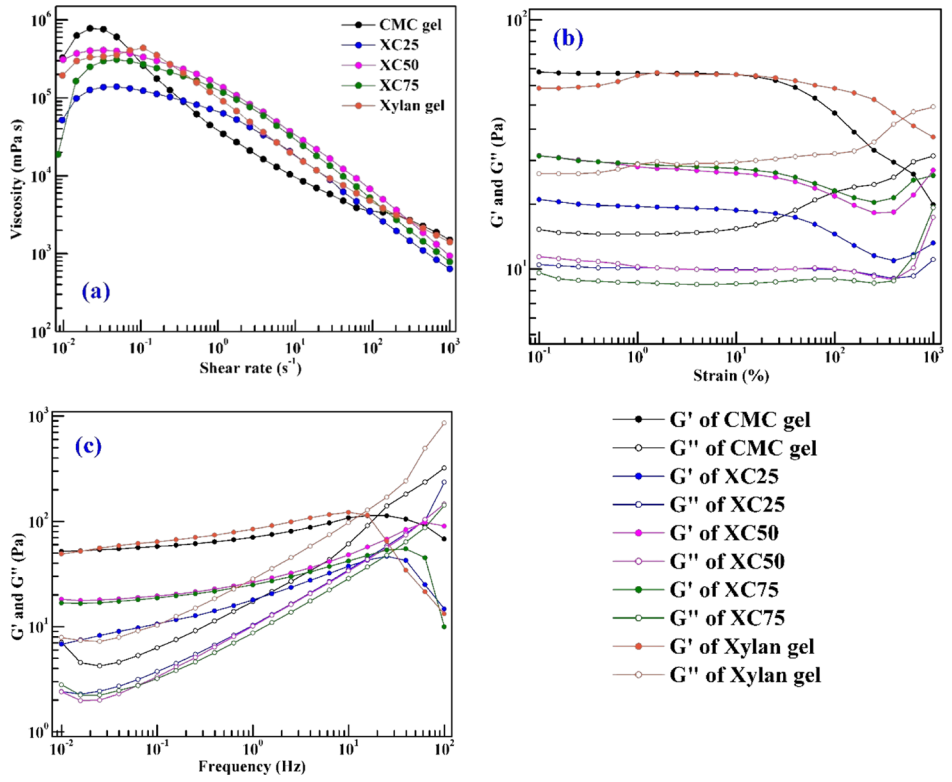

Figure 7. Rheology of hydrogels: (a) viscosity, (b) amplitude sweep, and (c) frequency sweep.

where η is the viscosity, $\dot{\gamma}$ is the shear rate, n is the power-law index, and m is the consistency index. The values of the parameters of the power-law model are given in Table 1. The

Table 1. Power-Law Parameters

name of the hydrogel	M	n	R^2
CMC gel	5.23×10^4	0.422	0.96
XC25	3.54×10^4	0.524	0.89
XC50	8.64×10^4	0.451	0.94
XC75	5.86×10^4	0.507	0.80
xylan gel	6.75×10^4	0.454	0.95

power-law index for all hydrogels is less than unity, which mathematically confirms the shear-thinning nature of gels with increasing shear rate. The goodness of fit is expressed in terms of correlation coefficient (R^2), the values of which are given in Table 1.

We further carried out the amplitude sweep test of the hydrogels to find out the storage and loss moduli of the gels. The amplitude sweep is reported in Figure 7b within the strain range of 0.1−1000% at 25 °C. For all gels, we observe a crossover at 500% of strain, and storage modules dominate over the loss modulus. The LVR is determined with 1% strain, and to confirm the viscoelastic characteristics, we performed the frequency sweep test, with a 1% strain constant. For the copolymerized gels, the dominance of storage modulus over the loss modulus reflects the solid-like behavior of the gels within the range of the strain considered. Figure 7c represents the frequency sweep plot of the gels at 25 °C, 1% strain, and 0.01−100 Hz frequency range. For all the gels, the dominance of storage moduli (G') is observed over the loss moduli (G'') until the crossover point, which typically appears after 10 Hz. Among all the gels, XC50 (50 mol % xylan/50 mol % CMC) shows the highest crossover frequency at 54.43 Hz which reflects that the structure of this gel can accommodate larger deformations than the pure CMC and xylan gels. For all the copolymerized gels, lesser values of storage and loss modulus have been observed than for the pure CMC and xylan gels. We have further calculated the loss tangent values of the hydrogels and plotted in Figure 8 as a log−log plot with

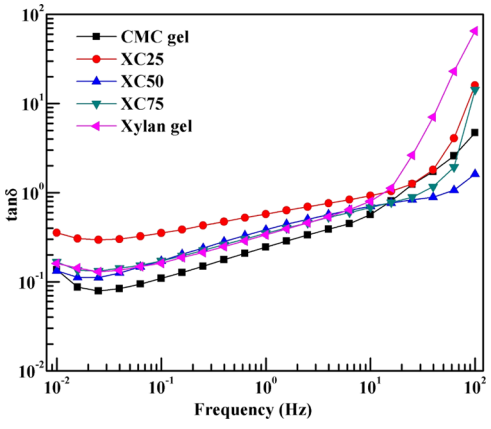

Figure 8. Loss tangent of hydrogels.

respect to the frequency. At higher frequencies (>10 Hz), the loss tangent becomes greater than unity, that is, a phase transition occurs. After the phase transition, the cross-linked structure breaks down, and thereafter the liquid-like behavior of the gels is confirmed.

Figure 9a represents the temperature sweep measurement of the precursors of hydrogels within 25−80 °C, with 1 °C min^{-1} increment of temperature, 1 Hz frequency, and 1% of strain. The gelation point, gelation temperature, and gelation time of all the hydrogels are given in Table 2. We observe that the viscous

DOI: 10.1021/acsomega.8b03671
ACS Omega 2019, 4, 4793−4803

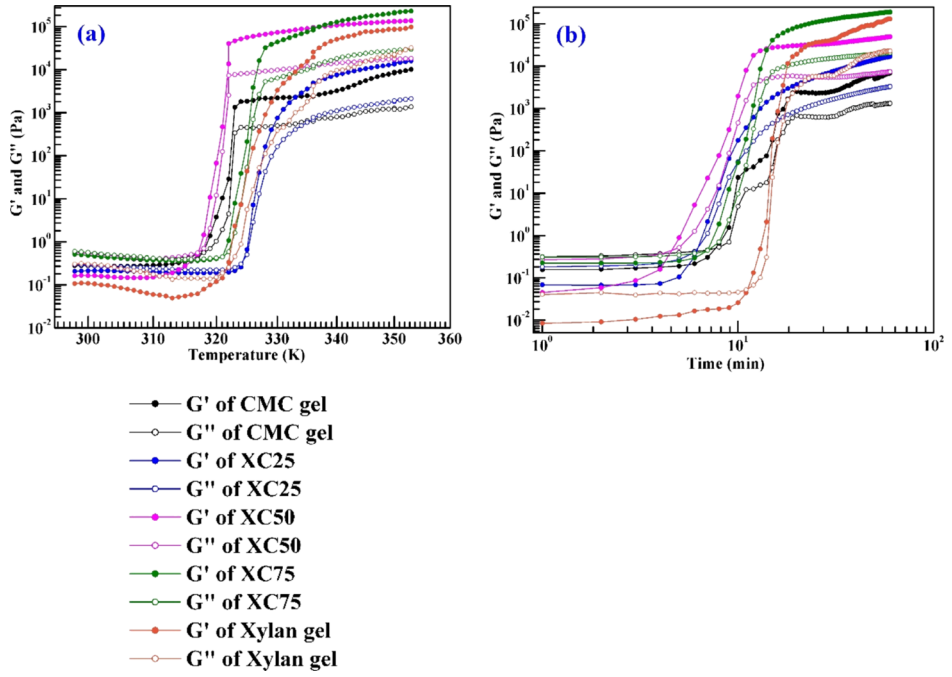

Figure 9. Temperature sweep and (b) time sweep of precursor solutions.

Table 2. Values of Gelation Parameters

	hydrogels				
parameters	CMC gel	XC25	XC50	XC75	xylan gel
gel point (Hz)	20.00	13.61	53.82	30.64	13.54
gelation temperature (K)	318	324	317	321	322
gelation time (min)	7.5	6.25	5	7	11

nature of the precursors dominates until the gelation temperature. The gelation temperature of all gels is observed within 317−324 K (43−51 °C). After the gelation temperature, elastic nature is seen to be prominent, that is, the evolution of network. During the evolution of network, a sharp rise in the storage and loss moduli is observed. The formation of the network is completed within 317−330 K (43−57 °C). The similar temperature range is also observed during the synthesis of the hydrogels. Among the five hydrogels, the XC50 gel has the narrowest temperature range for the network evolution. For this, 1:1 molar ratio is concluded as an ideal mixture to form the cellulose−hemicellulose hydrogel. After gelation, the network stabilizes, and no new crossover is observed. This implies that the stability of the network is up to 80 °C at LVR. Figure 9b represents the time sweep measurements of the precursor solutions measured at the corresponding gelation temperatures with 1 Hz frequency and 1% of strain. Like temperature sweep, the viscous nature of the precursor dominates until the crossover point. The crossover point for every hydrogel appears within 5−11 min, signifying the relative slow nature of gelation after the addition of the cross-linker. However, once it starts, the whole network is built up within 5−7 min, and sharp changes in the storage and loss moduli are observed. Among the five gels, XC50 provided the fastest gelation time of 5 min. After the evolution of network, the network remains stable for a long duration, which reflects its strong network formation and also confirms the elastic behavior when compared to the viscous behavior.

3.4. Swelling Ratio and Gel Fraction. Figure 10a represents the SR of hydrogels measured in DI water, AGF, AIF, and PBS buffers. Both CMC and xylan are linear polymers which create network gels by cross-linking. The dominant charge species of polysaccharides, that is, the hydroxyl moiety (in CMC and xylan) and carboxymethyl moiety (in CMC) repel each other and expand the network structure in a suitable medium. The SR is determined by the amount of water absorbed to the dry weight of the hydrogel. Here, the order of swelling is

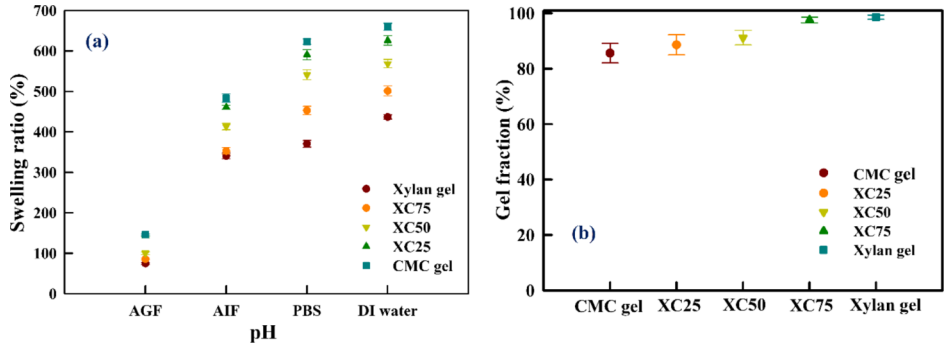

Figure 10. (a) SR of hydrogels in DI water and various buffers. (b) Gel fraction of hydrogels.

DOI: 10.1021/acsomega.8b03671
ACS Omega 2019, 4, 4793−4803

CMC gel > XC25 > XC50 > XC75 > xylan gel. The long-chain carboxymethyl moieties electrostatically repel each other; therefore the SR increases with the increment of the molar ratio of CMC in the hydrogel. Further, for all hydrogels, a greater swelling is observed in DI water. For buffers, the available free ions readily bind with the deprotonated hydroxyl and carboxymethyl moieties and hinder swelling. For this, least SR is observed in the AGF buffer. For all the hydrogels, the trend of SR observed in all buffers and DI water is: DI water > PBS > AIF > AGF. Figure 10b represents the gel fraction of the hydrogels. The gel fraction follows the trend: CMC gel < XC25 < XC50 < XC75 < xylan gel. As the gel fraction increases, the degree of cross-linking in the network increases. Therefore, the network has a less flexibility to swell and absorb more water. For this, the gel fraction follows the opposite trend of SR.[30]

3.5. Loading of VB_{12}. Figure 11 represents the VB_{12} loading in the hydrogels. The CMC gel and xylan gel have 15.46 and 17.75% VB_{12} loading, respectively, whereas the copolymerized gels have greater than 20% loading. XC50 has the highest VB_{12} loading of 36.59% among the copolymerized gels. The recorded loading is higher than that reported by Bajpai and Dubey[20] and Xu et al.[31] It is presumed that the porous structures of the copolymerized gels adsorb higher amounts of vitamin than the surface adsorption by pure CMC and xylan gels.

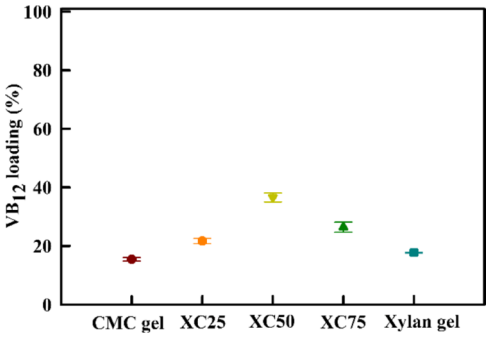

Figure 11. VB_{12} loading (%) in hydrogels.

3.6. In Vitro Release of VB_{12}. The in vitro release of VB_{12} from the hydrogel network in AGF, AIF, and PBS buffers is shown in Figure 12a–c. AGF mimics the stomach fluid, whereas AIF mimics the first zone of intestinal fluid.[32] The pH of the colonic fluid is 7.4 which is adequately represented by PBS.[33] Thus, the in vitro release of VB_{12} in these buffers will elucidate the vitamin release behavior in simulated physiological fluids. Further, Figure 12d represents the in vitro release of VB_{12} in consecutive buffers. The mean gastric emptying time is 1.08 h (±0.11 h) and the mean colonic arrival time is 2.83 h (±0.33 h), which reflect the transit time through the small intestine as 1.75 h (±0.25 h).[34] Therefore, the residence time of 2 h in the gastric fluid, that is, AGF, 2 h in the intestinal fluid, that is, AIF, and 6 h in the colonic fluid, that is, PBS would be a realistic effort to simulate the in vitro release of VB_{12} in the gastrointestinal tract.[33]

It is observed from Figure 12a–c that the in vitro release of VB_{12} depends on the pH of the medium. A cumulative release of less than 28% is observed in AGF compared to 80–88% in AIF and 93–98% in PBS. The release of guest molecules (here VB_{12}) from the hydrogels depends on the available ions in the buffer as well as the swelling nature of the hydrogels. The swelling of the hydrogels occurs because of the repulsion of the charged moieties which allow them to move away from each other, resulting in the loosening of the matrix, thereby allowing the diffusion of water. However, a lower swelling is observed if the negatively charged hydroxyl and carboxyl moieties are quickly protonated. Therefore, for AGF, higher amounts of the available H^+ ions quickly occupy the unprotonated sites and thus block the electrostatic repulsion and in turn lower the released amount of VB_{12}. The CMC and xylan gels release 19.05 and 19.27% VB_{12}, respectively, in the AGF buffer after 8 h, whereas the copolymerized gels release within 24–28%. A flat plateau is

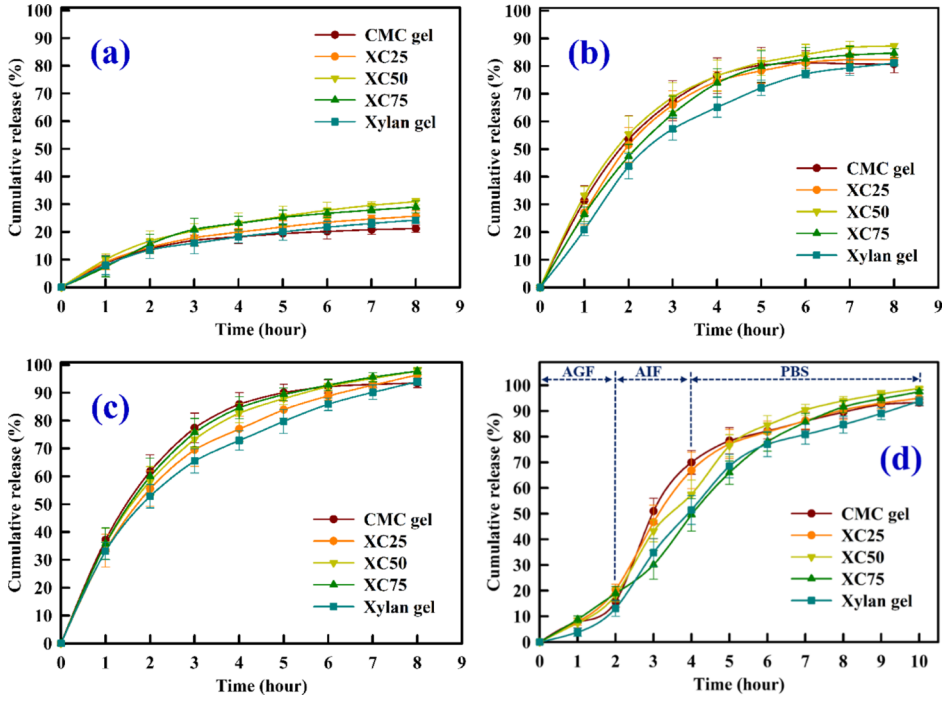

Figure 12. In vitro release of VB_{12} in physiological buffers: (a) AGF buffer, (b) AIF buffer, (c) PBS buffer, and (d) AGF–AIF–PBS buffer.

DOI: 10.1021/acsomega.8b03671
ACS Omega 2019, 4, 4793–4803

Table 3. Comparison With the Literature of In Vitro Release of VB_{12} Using Hydrogels

article	monomers	VB_{12}-loading concentration	release of VB_{12}	references
Boruah et al.	CMC-*g*-poly(acrylic acid) and organophilic montmorillonite nanoclay composite	0.125 wt % in buffer solution of pH = 7.0	55 and 34% cumulative release in 10 h for pH 7.4 and 1.2 respectively	22
Nath and Dolui	CMC-*g*-poly(acrylic acid) and LDH	1.25 wt % in buffer solution of pH = 7.0	released in pH = 1.2 and 7.4. 59 and 45% cumulative release in 6 h for pH 7.4 and 1.2, respectively, for that without LDH. With LDH, 66 and 50% cumulative release in 6 h for pH 7.4 and 1.2 respectively	23
Cao et al.	xylan-type hemicellulose	0.5 mg mL^{-1} aqueous solution	PBS buffer, with or without the presence of UV irradiation of 365 nm, at 37 ± 3 °C. Cumulative release is 89.3%	24
present study	CMC sodium salt and beechwood xylan	0.5 mg mL^{-1} aqueous solution	19−28% release in AGF, 80−88% release in AIF, and 93−98% release in PBS within 8 h at 37 °C. 93−99% release in consecutive physiological buffers within 10 h	

observed for all the release profiles in AGF, which reflects the tightly bound VB_{12} cannot be released in AGF. Only the loosely bound VB_{12} is released in AGF. In AIF and PBS, we observe an initial burst release of VB_{12} (Figure 12b,c). The burst release is attributed to the swelling behavior of the gels and dominates for the first 2 h for all gels. However, after the initial burst, we observe a slow and gradual release of VB_{12}. During this time, the ions of the respective buffers bind with the hydroxyl moieties, facilitating the release of VB_{12} into the medium. From Figure 12d, we observe a similar amount of VB_{12} release in AGF in first 2 h as compared to VB_{12} release in AGF only (Figure 12a). However, the burst releases in AIF and PBS are not observed here as the unprotonated moieties are already been occupied with H^+ ions from AGF. The release of VB_{12} will mainly depend on the available ions of the AIF and PBS buffers. Therefore, we observe that a significant amount of VB_{12} has been delivered in PBS, that is, the hydrogels are capable to release VB_{12} in the colon. Further, the hydrogels are also able to deliver VB_{12} for a longer duration of 10 h if they are first exposed to AGF.

The in vitro release study in the different physiological buffers also defines the efficiency of hydrogels as effective carriers of VB_{12}. In all release media, the XC50 hydrogel is proven to facilitate te highest cumulative release as compared to the other gels. Although the CMC and xylan gels produce the highest and lowest SRs in all buffers, respectively, the cumulative release is lower than that of the copolymerized gels. This indicates that the mere diffusion of water and the resulting relaxation of cross-linking are not the prime factors for the delivery of VB_{12}. The copolymeric gels have porous morphology as observed from FESEM, providing the ideal binding sites for VB_{12} both at the surface as well as inside the pores. Further, these gels have a higher gelation point, that is, they can withstand a high deformation strain than the pure CMC and xylan gels. Thus, they can better hold the cross-linked structure. Further, for longer duration, the VB_{12} molecules can be attached to the binding sites.

3.7. Comparison of In Vitro Release of VB_{12} with the Literature. The in vitro release of VB_{12} from the hydrogels in physiological buffers is then compared with the previously reported two CMC-based hydrogels and one xylan-based hydrogel. The summary of comparison is given in Table 3. Boruah et al. reported a less than 35% cumulative release of VB_{12} in pH 1.2 and less than 55% cumulative release of VB_{12} in pH 7.4 after 10 h using CMC-grafted poly(acrylic acid) and organophilic montmorillonite nanoclay composite hydrogel.[22] However, the cumulative release increases to 76.2% after 10 h using a lower amount of cross-linker in DI water at room temperature. Nath and Dolui reported VB_{12}-loaded CMC-grafted poly(acrylic acid) and LDH hydrogel.[23] The hydrogel released 66% VB_{12} in pH 7.4 and 50% in pH 1.2 in 6 h. They further reported that the VB_{12}-loaded hydrogel without LDH was seen to release a total of 45% in pH 1.2 and 59% in pH 7.4 after 6 h. Cao et al. also reported the in vitro release of VB_{12} from multiresponsive xylan hydrogels in pH 2.2 and 7.4 at 37 °C for a period of 7 h.[24] A cumulative release of 78.3% in acidic medium and 89.3% in alkaline medium without UV irradiation has been reported, whereas a higher amount of VB_{12} has been released in alkaline medium in the presence of UV. Compared to the previous reports, the CMC−xylan copolymerized hydrogels of this work have a higher delivery capacity in AIF and PBS, respectively, for a longer duration. However, a lesser amount of VB_{12} is delivered in the AGF medium. Unlike the previous reports, we have studied the delivery of VB_{12} in the consecutive physiological buffers of the gastrointestinal tract. Overall, the hydrogels are capable of delivering VB_{12} greater than 90% for 10 h.

4. CONCLUSIONS

EGDE-cross-linked CMC- and xylan-based homopolymerized hydrogels as well as copolymerized CMC−xylan-based gels are synthesized in an alkaline medium. Among the five gels, the CMC gel possesses the highest SR, and the xylan gel has the least SR in AGF, AIF, PBS buffer, and DI water. The SR of the CMC gel is 146.58% in AGF buffer which steadily increases to 659.34% in DI water. However, the gel fraction follows the opposite trend of SR, that is, a highest gel fraction of 98.63% is obtained with the xylan gel, whereas the CMC gel produces 85.64% gel fraction. The morphologies of the CMC and xylan gels appear to be coarse in nature, whereas the copolymerized CMC−xylan gels are porous in nature. All five hydrogels produce a shear-thinning behavior upon increasing the rate up to 1000 s^{-1}. Further, the CMC−xylan gel (1:1 molar ratio) gave a longer gel point than the CMC gel and xylan gel. The longer gel point proves that the copolymerized structure can withstand more stress than pure hydrogels. Further, the loss tangent values are less than unity until the gel point, signifying the elastic nature of the hydrogels which dominates over the viscous nature. The dominance of the elastic nature concludes the successful cross-linking with EGDE, whereby the hydrogels can relax the cross-linking structure up to the gel point with an influence of the external stimuli. The CMC−xylan gel (1:1 molar ratio) has the least gelation temperature of 317 K, and the gelation process starts after 5 min. After gelation, a stable hydrogel network is observed up to 80 °C. This hydrogel is further proved to have a higher VB_{12} loading of 36.59%. Further, the copolymerized gels release 24−28% VB_{12} in AGF, 82−88% in AIF, and 96−98% in PBS, which are higher than that of the homopolymerized gels. The in vitro release profile reflects the initial burst release of VB_{12} followed by the steady release up to 8 h.

DOI: 10.1021/acsomega.8b03671
ACS Omega 2019, 4, 4793−4803

■ ASSOCIATED CONTENT

Supporting Information

The Supporting Information is available free of charge on the ACS Publications website at DOI: 10.1021/acsomega.8b03671.

Structure of monomers and cross-linker and the plots for the amplitude sweep, frequency sweep, temperature sweep, and time sweep (PDF)

■ AUTHOR INFORMATION

Corresponding Author

*E-mail: tamalb@iitg.ac.in. Phone: +91 361 2582266. Fax: +91 361 2582291.

ORCID

Tamal Banerjee: 0000-0001-8624-6586

Notes

The authors declare no competing financial interest.

■ REFERENCES

(1) Ullah, F.; Othman, M. B. H.; Javed, F.; Ahmad, Z.; Akil, H. M. Classification, processing and application of hydrogels: A review. *Mater. Sci. Eng., C* **2015**, *57*, 414−433.

(2) Roy, N.; Saha, N.; Kitano, T.; Saha, P. Development and characterization of novel medicated hydrogels for wound dressing. *Soft Mater.* **2010**, *8*, 130−148.

(3) Sadiasa, A.; Franco, R. A.; Seo, H. S.; Lee, B. T. Hydroxyapatite delivery to dentine tubules using carboxymethyl cellulose dental hydrogel for treatment of dentine hypersensitivity. *J. Biomed. Sci. Eng.* **2013**, *06*, 987−995.

(4) Reza, A. T.; Nicoll, S. B. Characterization of novel photo-crosslinked carboxymethylcellulose hydrogels for encapsulation of nucleus pulposus cells. *Acta Biomater.* **2010**, *6*, 179−186.

(5) Dutta, S.; Samanta, P.; Dhara, D. Temperature, pH and redox responsive cellulose based hydrogels for protein delivery. *Int. J. Biol. Macromol.* **2016**, *87*, 92−100.

(6) Lee, S.; Park, Y. H.; Ki, C. S. Fabrication of PEG-carboxymethylcellulose hydrogel by thiol-norbornene photo-click chemistry. *Int. J. Biol. Macromol.* **2016**, *83*, 1−8.

(7) Chang, C.; Zhang, L. Cellulose-based hydrogels: Present status and application prospects. *Carbohydr. Polym.* **2011**, *84*, 40−53.

(8) Teleman, A.; Larsson, P. T.; Iversen, T. On the accessibility and structure of xylan in birch kraft pulp. *Cellulose* **2001**, *8*, 209−215.

(9) Deutschmann, R.; Dekker, R. F. H. From plant biomass to bio-based chemicals: Latest developments in xylan research. *Biotechnol. Adv.* **2012**, *30*, 1627−1640.

(10) Ebringerová, A.; Hromádková, Z. Xylans of industrial and biomedical importance. *Biotechnol. Genet. Eng. Rev.* **1999**, *16*, 325−346.

(11) Ebringerová, A.; Heinze, T. Xylan and xylan derivatives - biopolymers with valuable properties, 1. Naturally occurring xylans structures, isolation procedures and properties. *Macromol. Rapid Commun.* **2000**, *21*, 542−556.

(12) Sun, X.-F.; Wang, H.-H.; Jing, Z.-X.; Mohanathas, R. Hemicellulose-based pH-sensitive and biodegradable hydrogel for controlled drug delivery. *Carbohydr. Polym.* **2013**, *92*, 1357−1366.

(13) Dax, D.; Chávez, M. S.; Xu, C.; Willför, S.; Mendonça, R. T.; Sánchez, J. Cationic hemicellulose-based hydrogels for arsenic and chromium removal from aqueous solutions. *Carbohydr. Polym.* **2014**, *111*, 797−805.

(14) Sun, X.-F.; Gan, Z.; Jing, Z.; Wang, H.; Wang, D.; Jin, Y. Adsorption of methylene blue on hemicellulose-based stimuli-responsive porous hydrogel. *J. Appl. Polym. Sci.* **2015**, *132*, 41606.

(15) Pettenuzzo, A.; Pigot, R.; Ronconi, L. Vitamin B_{12}-Metal Conjugates for Targeted Chemotherapy and Diagnosis: Current Status and Future Prospects. *Eur. J. Inorg. Chem.* **2017**, *2017*, 1625−1638.

(16) Giedyk, M.; Goliszewska, K.; Gryko, D. Vitamin B_{12} catalysed reactions. *Chem. Soc. Rev.* **2015**, *44*, 3391−3404.

(17) Jin, L.; Lu, P.; You, H.; Chen, Q.; Dong, J. Vitamin B_{12} diffusion and binding in crosslinked poly(acrylic acid)s and poly(acrylic acid-co-N-vinyl pyrrolidinone)s. *Int. J. Pharm.* **2009**, *371*, 82−88.

(18) Okuda, K. Discovery of vitamin B_{12} in the liver and its absorption factor in the stomach: A historical review. *J. Gastroenterol. Hepatol.* **1999**, *14*, 301−308.

(19) Dengre, R.; Bajpai, M.; Bajpai, S. K. Release of vitamin B_{12} from poly(N-vinyl-2-pyrrolidone)-crosslinked polyacrylamide hydrogels: A kinetic study. *J. Appl. Polym. Sci.* **2000**, *76*, 1706−1714.

(20) Bajpai, S. K.; Dubey, S. In vitro dissolution studies for release of vitamin B_{12} from poly(N-vinyl-2-pyrrolidone-co-acrylic acid) hydrogels. *React. Funct. Polym.* **2005**, *62*, 93−104.

(21) Maheswari, B.; Jagadeesh Babu, P. E.; Agarwal, M. Role of N-vinyl-2-pyrrolidinone on the thermoresponsive behavior of PNIPAm hydrogel and its release kinetics using dye and vitamin-B_{12} as model drug. *J. Biomater. Sci., Polym. Ed.* **2014**, *25*, 269−286.

(22) Boruah, M.; Gogoi, P.; Manhar, A. K.; Khannam, M.; Mandal, M.; Dolui, S. K. Biocompatible carboxymethylcellulose-g-poly(acrylic acid)/OMMT nanocomposite hydrogel for in vitro release of vitamin B_{12}. *RSC Adv.* **2014**, *4*, 43865−43873.

(23) Nath, J.; Dolui, S. K. Synthesis of carboxymethyl cellulose-g-poly(acrylic acid)/LDH hydrogel for in vitro controlled release of vitamin B_{12}. *Appl. Clay Sci.* **2018**, *155*, 65−73.

(24) Cao, X.; Peng, X.; Zhong, L.; Sun, R. Multiresponsive hydrogels based on xylan-type hemicelluloses and photoisomerized azobenzene copolymer as drug delivery carrier. *J. Agric. Food Chem.* **2014**, *62*, 10000−10007.

(25) Alshehri, S. M.; Aldalbahi, A.; Al-hajji, A. B.; Chaudhary, A. A.; Panhuis, M. i. h.; Alhokbany, N.; Ahamad, T. Development of carboxymethyl cellulose-based hydrogel and nanosilver composite as antimicrobial agents for UTI pathogens. *Carbohydr. Polym.* **2016**, *138*, 229−236.

(26) Swamy, B. Y.; Yun, Y.-S. In vitro release of metformin from iron (III) cross-linked alginate-carboxymethyl cellulose hydrogel beads. *Int. J. Biol. Macromol.* **2015**, *77*, 114−119.

(27) Gao, X.; Cao, Y.; Song, X.; Zhang, Z.; Zhuang, X.; He, C.; Chen, X. Biodegradable, pH-responsive carboxymethyl cellulose/poly(acrylic acid) hydrogels for oral insulin delivery. *Macromol. Biosci.* **2014**, *14*, 565−575.

(28) Kono, H.; Onishi, K.; Nakamura, T. Characterization and bisphenol A adsorption capacity of β-cyclodextrin-carboxymethylcellulose-based hydrogels. *Carbohydr. Polym.* **2013**, *98*, 784−792.

(29) Sekkal, M.; Dincq, V.; Legrand, P.; Huvenne, J. P. Investigation of the glycosidic linkages in several oligosaccharides using FT-IR and FT Raman spectroscopies. *J. Mol. Struct.* **1995**, *349*, 349−352.

(30) Wang, L.-Y.; Wang, M.-J. Removal of Heavy Metal Ions by Poly(vinyl alcohol) and Carboxymethyl Cellulose Composite Hydrogels Prepared by a Freeze-Thaw Method. *ACS Sustainable Chem. Eng.* **2016**, *4*, 2830−2837.

(31) Xu, X.; Fu, S.; Wang, K.; Jia, W.; Guo, G.; Zheng, X.; Dong, P.; Guo, Q.; Qian, Z. Preparation and characterization of Vitamin-12 loaded biodegradable pH-sensitive microgels. *J. Microencapsulation* **2009**, *26*, 642−648.

(32) Barkhordari, S.; Yadollahi, M. Carboxymethyl cellulose capsulated layered double hydroxides/drug nanohybrids for Cephalexin oral delivery. *Appl. Clay Sci.* **2016**, *121-122*, 77−85.

(33) Bajpai, S. K.; Dubey, S. Modulation of dynamic release of vitamin B_2 from a model pH-sensitive terpolymeric hydrogel system. *Polym. Int.* **2004**, *53*, 2178−2187.

(34) Krishnaiah, Y. S. R.; Satyanarayana, S.; Rama Prasad, Y. V.; Narasimha Rao, S. Gamma scintigraphic studies on guar gum matrix tablets for colonic drug delivery in healthy human volunteers. *J. Controlled Release* **1998**, *55*, 245−252.

DOI: 10.1021/acsomega.8b03671
ACS Omega 2019, 4, 4793−4803